Atmospheric Environment 176 (2018) 30–39

Contents lists available at ScienceDirect

Atmospheric Environment

journal homepage: www.elsevier.com/locate/atmosenv

Characterising fifteen years of continuous atmospheric radon activity observations at Cape Point (South Africa)

R. Botha[a,e,*], C. Labuschagne[b], A.G. Williams[d], G. Bosman[e], E.-G. Brunke[b], A. Rossouw[c,f], R. Lindsay[a]

[a] Department of Physics, University of Western Cape, Private Bag X17, Bellville 7535, South Africa
[b] South African Weather Service, c/o CSIR, PO Box 320, Stellenbosch 7599, South Africa
[c] Flerov Laboratory of Nuclear Reactions, JINR, Joliot-Curie str. 6, Dubna 141980, Russia
[d] Australian Nuclear Science and Technology Organisation, Locked Bag 2001, Kirrawee DC, NSW 2232, Australia
[e] Department of Physics, Stellenbosch University, Private Bag X1, Matieland 7601, South Africa
[f] Department of E & E Engineering, Stellenbosch University, Private Bag X1, Matieland 7601, South Africa

ARTICLE INFO

Keywords:
Radon
Inter-annual trend
Seasonal cycle
Periodicity
South Africa

ABSTRACT

This paper describes and discusses fifteen years (1999–2013) of continuous hourly atmospheric radon (^{222}Rn) monitoring at the coastal low-altitude Southern Hemisphere Cape Point Station in South Africa. A strong seasonal cycle is evident in the observed radon concentrations, with maxima during the winter months, when air masses arriving at the Cape Point station from over the African continental surface are more frequently observed, and minima during the summer months, when an oceanic fetch is predominant. An atmospheric mean radon activity concentration of 676 ± 2 mBq/m^3 is found over the 15-year record, having a strongly skewed distribution that exhibits a large number of events falling into a compact range of low values (corresponding to oceanic air masses), and a smaller number of events with high radon values spread over a wide range (corresponding to continental air masses). The mean radon concentration from continental air masses (1 004 ± 6 mBq/m^3) is about two times higher compared to oceanic air masses (479 ± 3 mBq/m^3). The number of atmospheric radon events observed is strongly dependent on the wind direction. A power spectral Fast Fourier Transform analysis of the 15-year radon time series reveals prominent peaks at semi-diurnal, diurnal and annual timescales. Two inter-annual radon periodicities have been established, the diurnal 0.98 ± 0.04 day^{-1} and half-diurnal 2.07 ± 0.15 day^{-1}. The annual peak reflects major seasonal changes in the patterns of offshore versus onshore flow associated with regional/hemispheric circulation patterns, whereas the diurnal and semi-diurnal peaks together reflect the influence of local nocturnal radon build-up over land, and the interplay between mesoscale sea/land breezes. The winter-time diurnal radon concentration had a significant decrease of about 200 mBq/m^3 (17%) while the summer-time diurnal radon concentration revealed nearly no changes. A slow decline in the higher radon percentiles (75th and 95th) for the winter and spring seasons is found over the 15-year data set, with most of the change occurring in the first 9 years (1999–2007). This observed inter-annual decline appears to be associated with changes in the frequency of air masses having originated from over the African continental surfaces, and no significant trend is found in the lower radon percentiles associated with oceanic air masses. The general decrease of atmospheric radon-associated with continental air-masses at Cape Point could be attributed to changing meteorological conditions, possibly driven by climate change.

1. Introduction

^{222}Rn (hereafter referred to as radon) is a naturally occurring noble gas, mostly of continental origin, frequently used for atmospheric tracer studies (Zahorowski et al., 2004; Crawford et al., 2009; Chambers et al., 2011; Williams et al.,2011). Radon is a radioactive α-decay product of long-lived ^{226}Ra ($t_{1/2}$ = 1 600 y), ubiquitous in most rock and soil types (Botha et al., 2017). Radon has a relatively consistent flux from ice-free terrestrial surfaces of 15–25 mBq m^{-2} s^{-1} varying mainly with soil characteristics such as composition, porosity, moisture and permeability (Ball et al., 1991; Griffiths et al., 2010; Karstens et al., 2015). The radon flux density from ice-free marine surfaces is two to three orders of magnitude smaller than that of continental regions (Schery and Huang, 2004; Zahorowski et al., 2013). As a result of these source

* Corresponding author. Department of Physics, University of Western Cape, Private Bag X17, Bellville 7535, South Africa.
E-mail address: rbotha@caretac.com (R. Botha).

https://doi.org/10.1016/j.atmosenv.2017.12.010
Received 2 October 2017; Received in revised form 8 December 2017; Accepted 11 December 2017
Available online 14 December 2017
1352-2310/ © 2017 Elsevier Ltd. All rights reserved.

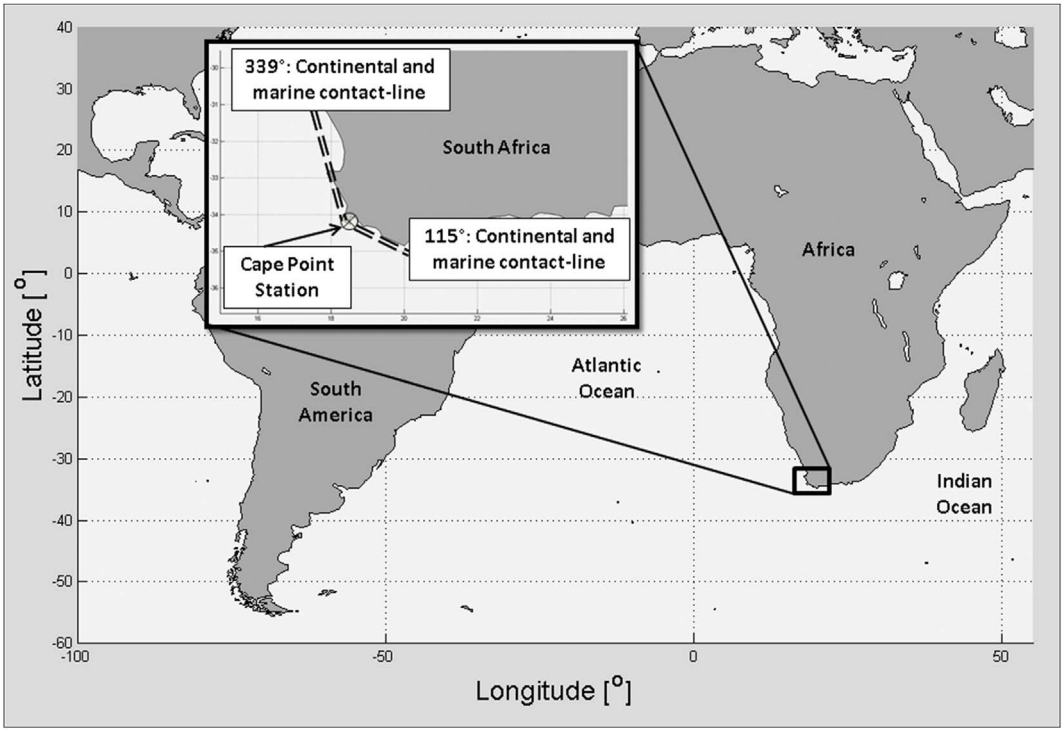

Fig. 1. Map indicates the location of the Cape Point Station. Two directional lines were inserted to indicate contact zones between continental and marine air masses regions.

characteristics, together with its unreactive nature and a radioactive half-life of 3.82 days, radon is an effective natural tracer by which continental air can be distinguished from marine air due to large activity concentration differences existing between the two air mass regimes (Brunke et al., 2004; Chambers et al., 2016).

At coastal baseline stations such as the Cape Point Global Atmospheric Watch (GAW) Station in South Africa, both continental and marine air masses are experienced (Fig. 1). Atmospheric radon measurements at Cape Point (CPT) have been utilised in various studies, including air-mass origin characterisation (Brunke et al., 2004); CO_2 source region identification for assessment via modelling studies; ^{222}Rn and meteorological data correlation studies (Brunke et al., 2004); and the characterisation of trace-gas source regions (Whittlestone et al., 2009). In this paper, we summarize the characteristics of, and trends in, a newly compiled fifteen-year data set (1999–2013) of continuous hourly atmospheric radon observations at the Cape Point Station (CPT), in conjunction with associated meteorological measurements.

2. Methods and measurements

2.1. Site description

Various baseline atmospheric measurements are routinely performed at the coastal Cape Point Station, under the South African Weather Service (SAWS) management. The Cape Point Station is situated within a nature reserve about 60 km south of Cape Town at the southernmost tip of the Cape Peninsula (see Fig. 1). The station is part of the Global Atmospheric Watch (GAW) network of baseline stations, functioning under the auspices of the World Meteorological Organization (WMO). The station is located at an altitude of 230 m above sea level on a coastal cliff (S 34.353 211° and E 18.489 683°). A range of continuous trace-gas measurements have been performed at the Cape Point Station (including CO, CO_2, CH_4, O_3, N_2O, and halocarbons) for the past 30 years (Brunke et al., 2004). More recently atmospheric radon and gaseous elemental mercury (GEM) has also been added to the list of continuous measurements (Slemr et al., 2013).

2.2. Radon measurement instrumentation

Since 1999, the Australian Nuclear Science and Technology Organisation (ANSTO) designed detector have been continuously measuring hourly atmospheric radon concentration levels at the Cape Point Station. The metrology and performance features of the ANSTO-built two flow-loop, dual-filter detectors have been well characterised in previous publications (e.g. Whittlestone and Zahorowski, 1998; Brunke et al., 2004; Chambers et al., 2011; Griffiths et al., 2016). Incremental improvements in the detection sensitivity of the Cape Point Station radon instrument resulted in a lower limit of detection (LLD) that reduced from an initial 42 ± 13 mBq/m^3 down to 33 ± 10 mBq/m^3 by 2001 (Brunke et al., 2004). In 2011, an upgraded version of the radon detector was installed, incorporating numerous system design improvements including an automated calibration system and a delay volume designed to further reduce potential thoron in-air within the detection chamber. This detector upgrade resulted in further improvements to the accuracy and reliability of the radon-in-air activity concentration measurements at Cape Point, with a new LLD of 25 ± 8 mBq/m^3.

The radon detector's sample inlet is located 30 m above ground level on an aluminium mast overlooking the coastal cliff at the Cape Point Station. The current detection system has a radon activity concentration measurement resolution of 30 min, which is further processed to an average 1-h temporal resolution. Instrumental background counts (accumulation of ^{210}Pb on the detector's second air filter) are measured on a three-month basis. The standard deviation of these background activity measurements is equivalent to 5 mBq/m^3 (Brunke et al., 2004). The radon concentration uncertainty for hourly measurements, taking into consideration the standard deviation of monthly calibration estimates (~2%) and the ± 4% accuracy of the calibration source, is of the order of 15% at 100 mBq/m^3 and 9% at 1 000 mBq/m^3 (Chambers et al., 2014).

2.3. Wind measurement instrumentation

Meteorological measurements made on top of the aluminium mast

at the Cape Point Station were used to identify the wind direction (WD). The air masses arriving at the Cape Point Station are frequently subjected to complex airflow patterns associated with the jagged terrain of the protruding cliff face where the station is situated (Brunke et al., 2004; Whittlestone et al., 2009). Airflow was classified (see Fig. 1) as predominantly of a continental nature within the WD angular distribution from 339° to 115°, clockwise. Two "mixed zones" were identified where continental and marine air masses potentially come into contact and mix, namely 115°–150° and 250°–339°. The remaining sector is referred to as "marine": 115°–339° with predominant associated marine air masses. Furthermore, a "deep baseline" was established between 180° and 273° associated almost entirely of marine air masses.

Measurement events with a wind speed (WS) of less than $^{5\ ms\text{-}1}$ were filtered out during our analyses to ensure that (1) nearby localised terrestrial radon emanations did not affect the baseline measurements and (2) to eliminate potentially inaccurate WD data associated with periods of calm wind conditions.

3. Results and discussion

3.1. Temporal characterisation of the Cape Point radon record

3.1.1. Time series and distributions

The atmospheric radon time series temporal characterization will highlight diurnal, monthly, seasonal and annual periodicities. The fifteen year (1999–2013) record shown in Fig. 2 exhibits a clear annual cycle, with a maximum during the austral winter and a minimum during the austral summer (see also Fig. 6). As will be seen in Section 3.2, the winter maximum is due to a higher incidence of continental air flow towards Cape Point during this season. Continental air masses are associated with higher radon levels when compared to marine air masses, due to significantly higher (2-3 orders of magnitude) radon fluxes from terrestrial surfaces (Brunke et al., 2004; Florea and Duliu, 2012). The 15-year median atmospheric radon level of 345 mBq/m^3 at the Cape Point Station is significantly lower. These differences likely indicate a greater overall continental influence at these coastal sites compared to Cape Point, when all seasons and wind directions are treated together. Moving inland from the continental edge, low-altitude surface sites typically exhibit average radon concentrations that are much higher again; for example, mean radon values at Lucas Heights, 20 km from the Australian east coast, are around 2 120 mBq/m^3 (Chambers et al., 2011), whilst in Arad, Romania, they have been reported by Florea and Duliu (2012) to be as high as 8 100 mBq/m^3. In contrast, mean values of radon observed at the remote island GAW site of Mauna Loa in Hawaii are 156 mBq/m^3 (Chambers et al., 2013).

The atmospheric radon distributions detected at Cape Point Station are profoundly skewed (Fig. 3 and Table 1), with data points between the 5th and 50th percentiles exhibiting a range of 289 mBq/m^3 (52–345 mBq/m^3), whereas those between the 50th and 95th percentiles have a range of 2 262 mBq/m^3 (345–2 603 mBq/m^3). The largest radon fluctuations are observed from the 75th and 95th radon percentiles. Also evident in Fig. 3 is an interesting characteristic that, the inter-annual 50th radon percentiles (median) of 345 mBq/m^3 can be considered relatively unchanged (STD 21 mBq/m^3) from 1999 to 2013. The 25th radon percentile was similarly mostly unchanged on an annual basis. However, the 75th and 95th radon percentiles appear to show a systematically declining trend over the years, with most of the change occurring in the first 6 years (1999–2005). This feature will be explored in more detail below.

3.1.2. Spectral analysis

Periodicities in the atmospheric radon signal were studied by computing a Fast Fourier Transform (FFT) power spectrum from the entire fifteen years of atmospheric radon signal (Fig. 4). A modest half-diurnal (0.5 days) and prominent diurnal (1 day) peaks are identifiable in the power spectrum (Fig. 4), followed by a variance that grows steadily up to about 10 days. The half-diurnal radon peak was further investigated and confidently confirmed from the inter-annual power spectrum analyses (see below, Fig. 5, lower and Fig. 9). The diurnal and 1–10 day radon periodicities are probably associated with various mesoscale flows that mix the ocean and continental air in and around the coastal region. A long plateau of high variances is visible from 10 to 300 days, likely corresponding to a range of synoptic and seasonal circulations that direct continental and

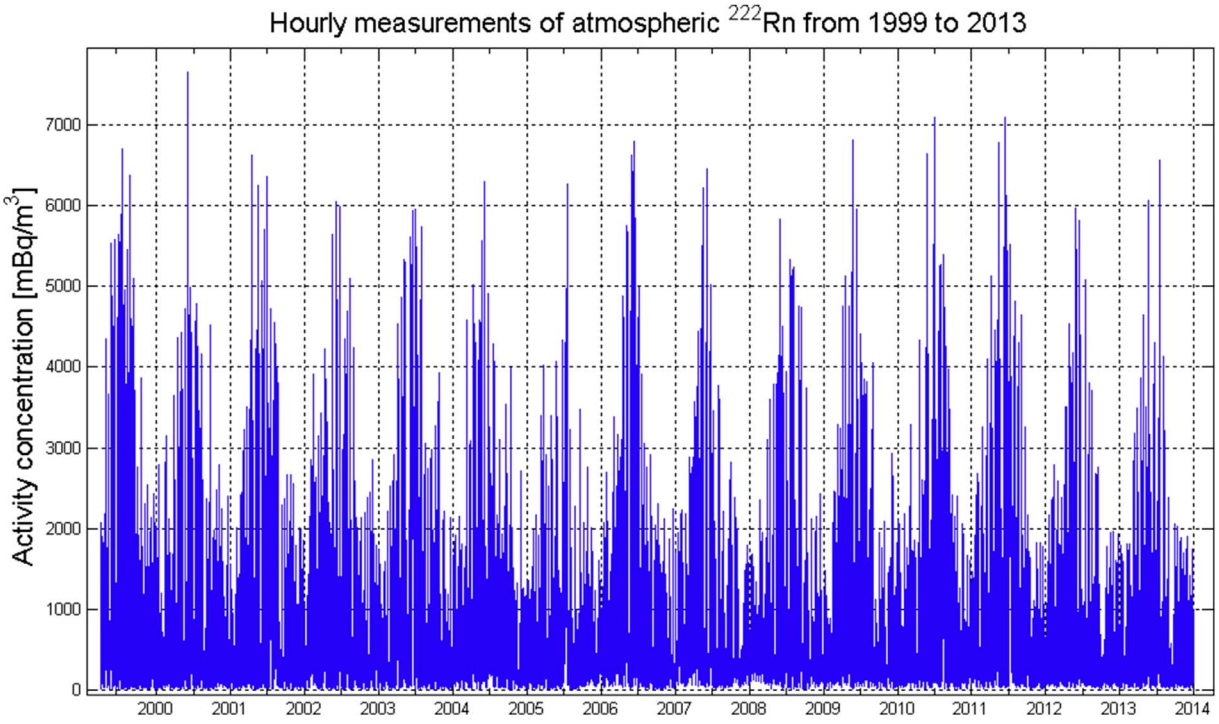

Fig. 2. 15-years of hourly atmospheric radon concentrations of Cape Point Station in South Africa.

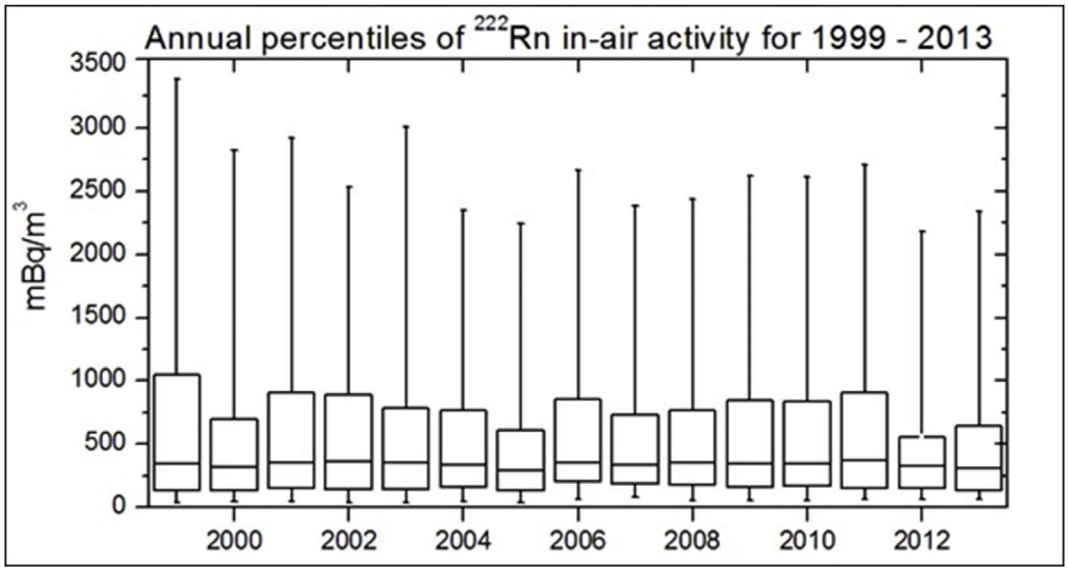

Fig. 3. Inter-annual atmospheric radon concentration distribution. The radon distribution is characterised by the whiskers, bars and central horizontal line within the bars which refer to 5th/95th, 25th/75th and 50th (median) percentiles, respectively.

Table 1
Radon concentration distributions of Cape Point from 1999 to 2013 and Cape Grim 2000 to 2011 (adapted from Zahorowski et al., 2013).

Station	5th percentiles, [mBq/m^3]	25th percentiles, [mBq/m^3]	50th percentiles, [mBq/m^3]	75th percentile, [mBq/m^3]	95th percentile, [mBq/m^3]	Mean, [mBq/m^3]
Cape Point	52	155	345	778	2 603	676
Cape Grim	14	42	141	593	3 003	595

ocean air masses across the coast. Finally, a large peak centered on 365 days corresponds to the annual cycle of regional/hemispheric seasonal circulations. This annual peak reflects major seasonal changes in the patterns of offshore versus onshore flow associated with regional/hemispheric circulation patterns. Seasonal patterns will be explored further below and in Section 3.2.

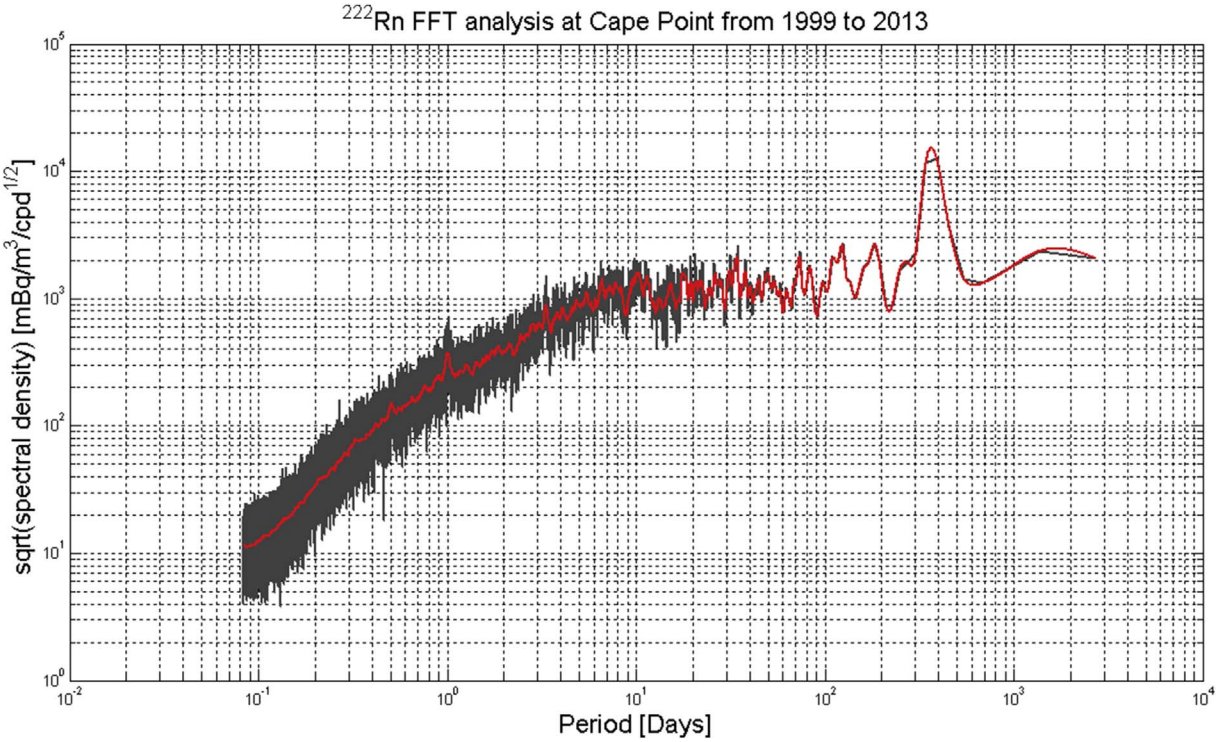

Fig. 4. Amplitude of the power spectrum for the entire 15-year radon time series using a FFT analysis (cpd, counts per day). The grey-line represents the raw power spectrum and the red-line the smoothed spectrum processed using Savitzky-Golay digital filtering. (For interpretation of the references to colour in this figure legend, the reader is referred to the Web version of this article.)

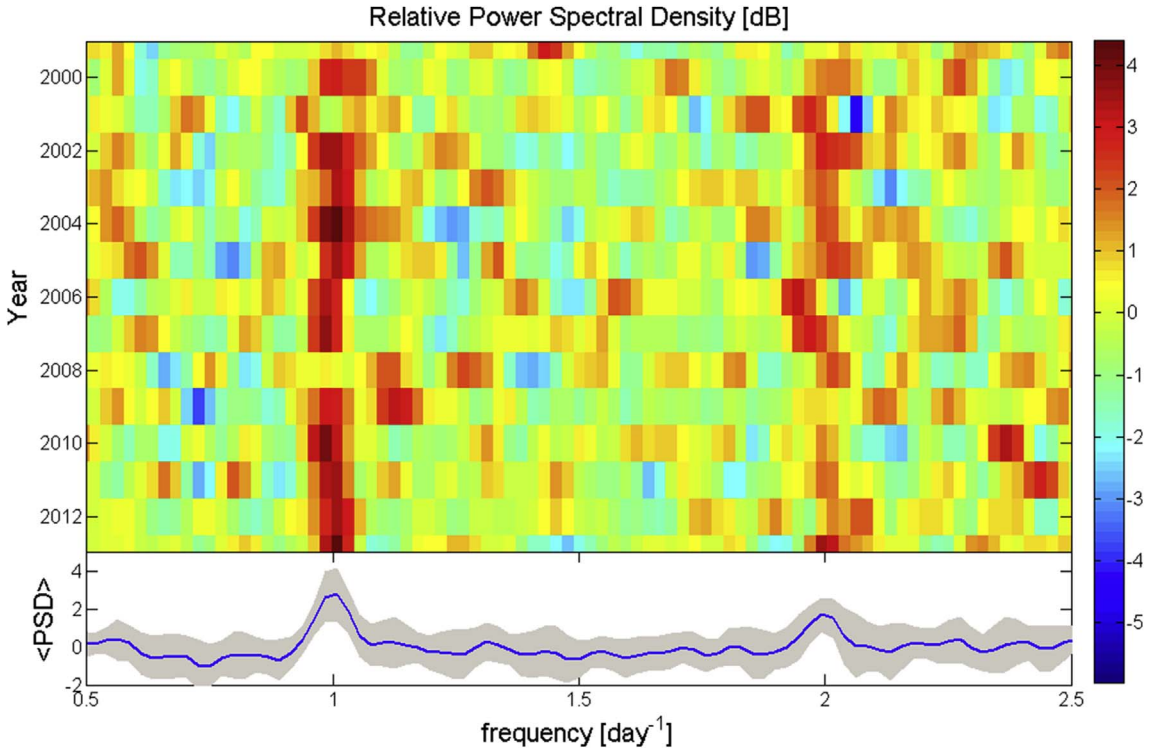

Fig. 5. The relative inter-annual atmospheric radon power spectral density (PSD) from 1999 to 2013 (upper) and the averaged PSD for the same period (lower, blue line – mean, grey area - standard deviation). (For interpretation of the references to colour in this figure legend, the reader is referred to the Web version of this article.)

The diurnal and semi-diurnal peaks together reflect the influence of local nocturnal radon build-up over land, possibly modulated by interplay between mesoscale sea/land breezes. It is well known that the nocturnal build-up of radon concentrations over land often leads to a ramp-shaped diurnal radon signal (Chambers et al., 2011). The presence of a ramp-shaped structure in the diurnal radon signal is confirmed in Fig. 9 (Section 3.2). When such a pattern (like a skewed sine wave of period 1 day) is repeated frequently enough in a time series such as in Fig. 2, a FFT analysis would display it as a family of spectral peaks at multiples of the diurnal frequency.

To explore this aspect a little further, FFT analysis of the radon time-series was also performed on an inter-annual basis, focusing on the shorter timescales (Fig. 5). The radon time series were binned into the respective individual years and power spectra were then computed up to timescales of 2 days. Clear periodicities were identified with frequencies of 1.02 ± 0.04 day^{-1} (diurnal) and 2.07 ± 0.15 day^{-1} (half-diurnal), consistent from year to year apart from in 2001 and 2008.

3.1.3. Seasonal characteristics

Monthly radon percentile distributions compiled from the 15-year data set (Fig. 6) show that elevated atmospheric radon activity concentrations are predominantly observed during the austral autumn (Mar, Apr and May) and winter months (June, July and Aug). More specifically, autumn and winter have 75th percentiles of atmospheric radon in the range 800–1 600 mBq/m^3 and 95th percentiles in the range 2000–4 000 mBq/m^3, whilst in the spring (Sept, Oct and Nov) and summer (Dec, Jan and Feb) 75th percentiles are in the range 400–600 mBq/m^3 and 95th percentiles are in the range 1 100–1800 mBq/m^3. These results indicate a dominance of continental air masses in the autumn and winter. On the other hand, the lower percentile ranges (below the median) exhibit comparatively less variability across the year, with the 5th and 25th percentiles (< ~200 mBq/m^3) having practically no seasonal and monthly temporal variations. Generally low atmospheric radon (< 500 mBq/m^3) indicates air masses of oceanic and mixed continental/ocean origin, whilst events falling below 150 mBq/m^3 correspond to air masses that have spent considerable time (1–2 weeks) exclusively over marine fetch regions (Brunke et al., 2004; Whittlestone et al., 2009) and away from land (so-called baseline periods).

These observed Southern Hemisphere radon distributions and seasonal atmospheric radon characteristics at Cape Point Station (South Africa) are similar to observations made at the Cape Grim Station in Tasmania, Australia (Zahorowski et al., 2013). The similarities include a seasonal WD shift leading to experiencing predominantly oceanic air masses in the austral summer months to a more frequent occurrence of continental air masses during the austral winter months.

Cape Grim's 5th to 25th radon percentiles are approximately four times lower than the corresponding Cape Point percentiles (see Table 1). This is mainly as a result of the pristine oceanic fetch region (< 40S) surrounding the Australian station and the longer oceanic residence time of arriving air masses to the station. The 50th radon percentile observed at Cape Point Station is approximately twice that of Cape Grim and can be explained by the occasional re-circulation of continentally influenced air masses found at the Cape Point Station. The 75th and 95th radon percentiles difference are smaller for the two stations, indicating possible similar continentally derived conditions.

Fig. 7 represents inter-annual trends in the percentile distributions, separated into seasons. For the winter (JJA) season, the composite 75th and 95th radon percentiles show a marked decrease (46% and 21%, respectively) over the 15 years, with most of the change occurring in the first 9 years (before 2007). In spring (SON), a similar trend is seen (75th and 95th percentiles decreased by 33% and 26%, respectively). It is evident that the higher atmospheric radon percentiles did decrease on an annual basis for the winter and spring seasons during this study (see Fig. 7). No significant composite atmospheric radon variations were observed in the lower percentiles (5th, 25th and 50th) for all the seasons which are usually associated with oceanic air and mixed masses.

The inter-annual declining trend as seen in the combined data set (Fig. 3) and highlighted in the upper percentiles in Fig. 7, relates to a

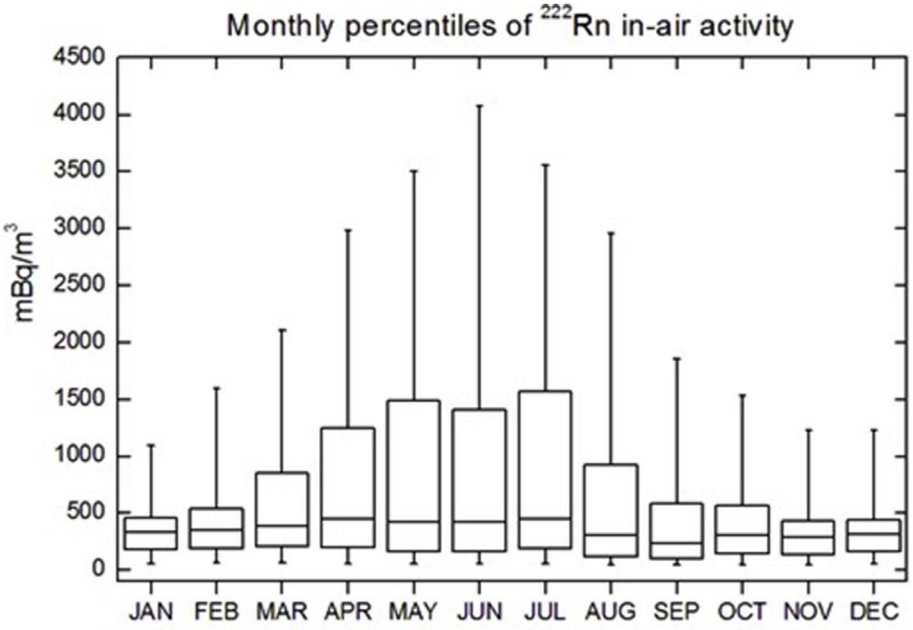

Fig. 6. 15-year monthly radon concentration distribution. The radon distribution is characterised by the whiskers, bars and central horizontal line within the bars which refer to 5th/95th, 25th/75th and 50th (median) percentiles, respectively.

specific wind sector and season. Since this occurrence is confined to the higher percentiles in winter and spring, an investigation into those specific transportation pathways were done. As will be seen in the next section, this trend appears to be associated with changes in the frequency of air masses arriving at Cape Point from over the African continental surface.

3.2. Radon and meteorological characterization

The atmospheric radon time-series at Cape Point Station was additionally characterized according to the wind direction (WD) and wind speed (WS). The relationship between atmospheric radon and wind in the Cape Point data set is illustrated in Fig. 8. WD sectors with predominantly lower atmospheric radon concentrations correspond as

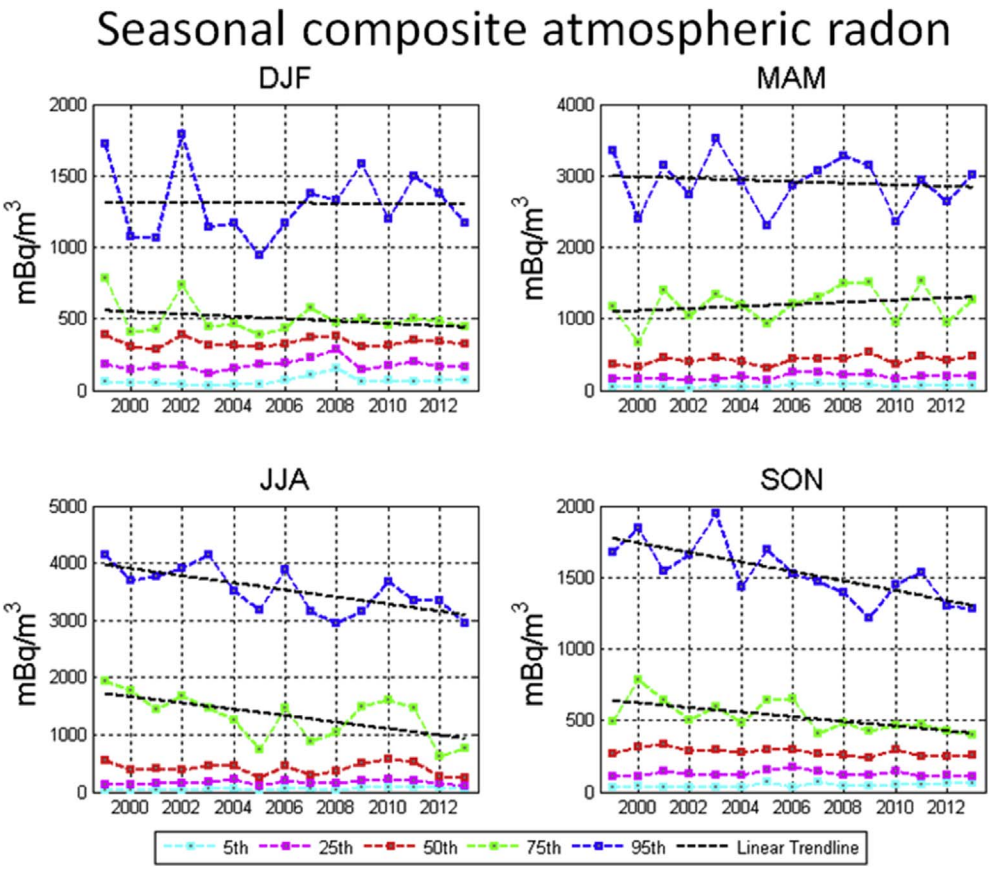

Fig. 7. Inter-annual variations in seasonal atmospheric radon distributions. The radon distributions are characterised by 5th, 25th, 50th, 75th and 95th percentiles with associated simple linear regressions.

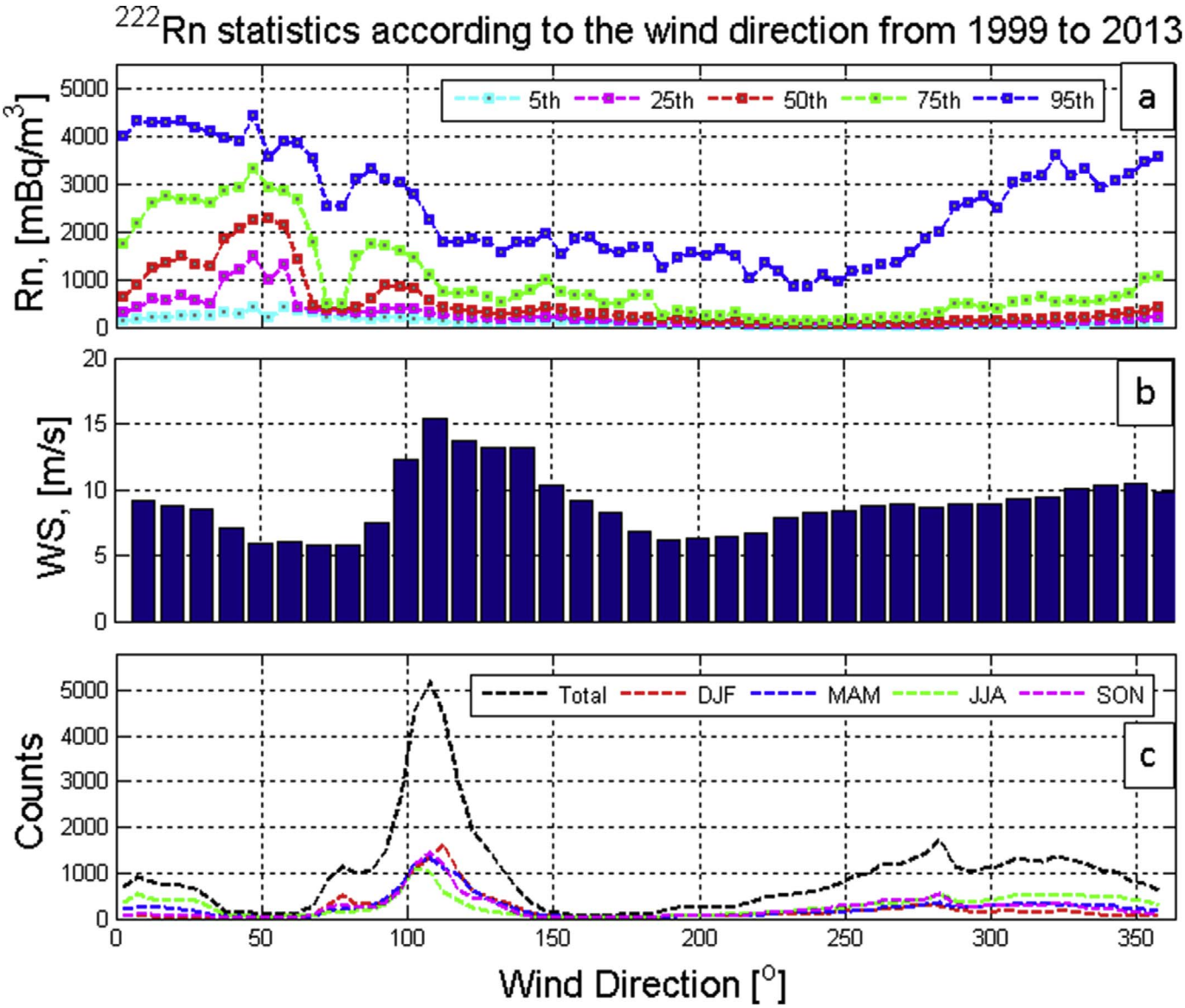

Fig. 8. WD-dependence of: (a) atmospheric radon distribution; (b) mean wind speed; and (c) number of radon events by season. The radon distribution in (a) is characterised by 5th, 25th, 50th, 75th and 95th percentiles.

expected to the geographical oceanic regions: 40°–80° (False Bay) and 115°–339° (Atlantic and Indian Ocean). The lowest radon concentrations are found in the sub-sector 188°–273°, corresponding to "deep baseline" events. A radon concentration peak occurs in all the percentiles at a WD of 48°, which coincides with the centre of the continental fetch region (see Fig. 1). An elevated number of radon events (> 1 000 counts) did not coincide (Fig. 8) with an elevated median atmospheric radon activity concentration (> 1 000 Bq/m^3).

The highest number of atmospheric radon events (Fig. 8c) occurred in a WD band around 109°, which corresponds with the mixing zone (M1) between African continental air masses and Indian Ocean air masses. The highest average WS (Fig. 8b) coincides with the highest number of total atmospheric radon events (Fig. 8c) with respect to the identical WD band (100° to 140°). The number of atmospheric radon events observed is strongly dependent on the WD which is applicable to all the seasons (Fig. 8c). No specific season's associated number of atmospheric radon events can be considered as predominant for the entire WD band (Fig. 8c). The number of atmospheric radon events associated with the winter (JJA) is predominant over the summer (DJF) for the WD band of 206° to 65° (clockwise, Fig. 8c). The mean atmospheric radon decreased at a linear rate of about 12 mBq/m^3 for every 1 m s^{-1} increase in the wind speed for the 15-year radon time series. The decrease in the mean atmospheric radon as the wind speed increases can be expected based on that most atmospheric radon events (53%) detected are associated with marine air masses (Fig. 8c).

Fig. 9 examines the diurnal dependence of radon with wind speed (WS) and direction (WD). The ramp-shaped signal visible in the radon diurnal composite (Fig. 9a), starting in the late afternoon (~19:00) and increasing to a maximum in the mid-morning (~10:00), is a well-known characteristic of the regional nocturnal build-up of radon over land (Chambers et al., 2011). As discussed in Section 3.1, the asymmetric shape of this curve is the cause of the diurnal and semi-diurnal peaks in the radon power spectrum (Fig. 5). Most of the variability in the diurnal radon signal originates from the higher percentiles, which tend to be associated with terrestrial influences (Fig. 9a). Fig. 9b presents the mean radon diurnal signal distributions, separated into

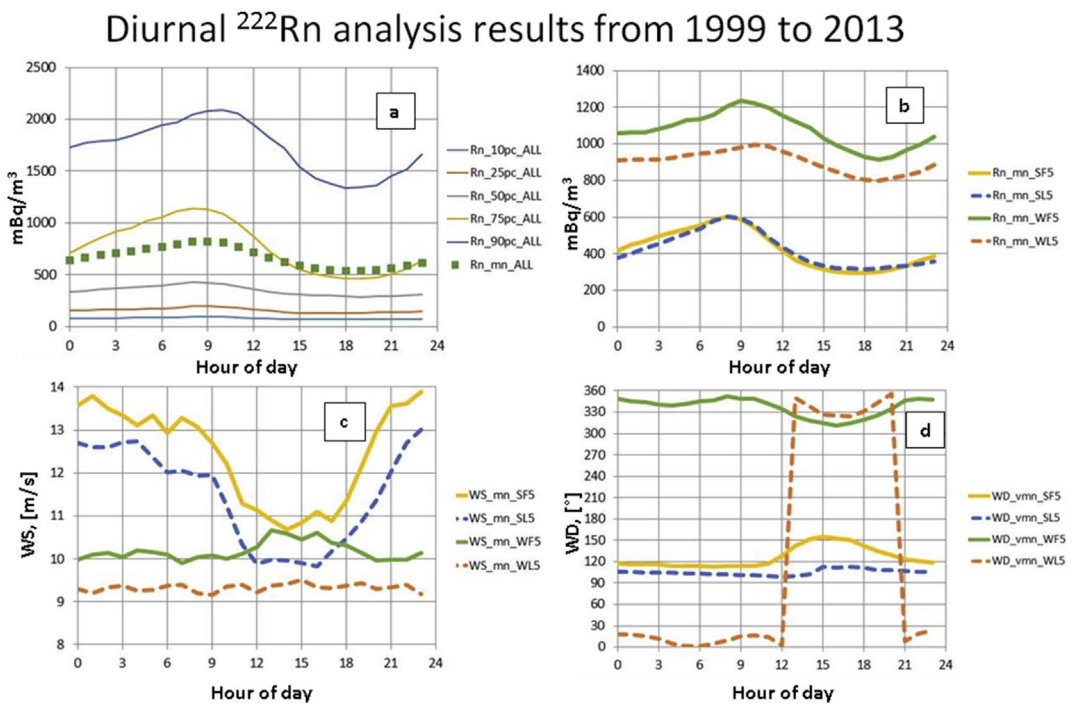

Fig. 9. Diurnal composites of: (a) radon and its distribution (mean values, as well as 10th, 25th, 50th, 75th and 90th percentiles) for the whole data set; (b) mean radon separated into summer (S) and winter (W) curves for the first (F5) and last (L5) 5 years of the data set; (c) mean scalar wind speed; and (d) vector mean wind direction.

Table 2
Mean and median atmospheric radon concentrations at Cape Point from 1999 to 2013, categorised according to distinct WD sectors.

Air mass sector	Mean atmospheric radon levels, [mBq/m^3]	Median atmospheric radon levels, [mBq/m^3]
Marine MA1 (115°–339°)	479 ± 3	173
Continental C1 (339°–115°)	1 004 ± 6	567
Mixed M1 (100°–150°)	725 ± 5	450
Mixed M2 (250°–339°)	493 ± 3	136
Deep Baseline DB1 (180°–273°)	279 ± 3	94

summer (S)- and winter (W)-only curves for the first (< = 2003, F5) and last (> = 2009, L5) 5 years of the data set. As discussed previously, winter radon levels are significantly higher than summer, due to the increased frequency of continental air masses. This is confirmed in Fig. 9c and d, which show that whereas summer winds are generally faster and from the SE (slowing and turning further south in the afternoon), the winter winds tend to be slower and from the NNW (influenced more by the "Berg wind").

A fascinating feature of Fig. 9b is that, whereas there has been the microscopic change in the summer-time diurnal cycle of radon, the winter-time cycle has significantly dropped in value over the entire diurnal period. The largest decrease (17%) in the summer-time diurnal cycle of radon occurred near the mid-morning maximum and was around 200 mBq/m^3. This coincides with a clear drop in wind speeds over the entire diurnal cycle, and a shift in direction from NNW towards northerlies or even NNE (Fig. 9c and d).

Table 2 presents the atmospheric radon time-series characterisation according to the four distinct WD regions discussed above (see also Section 2.3). The mean atmospheric radon concentrations for predominantly marine fetch regions (MA1; 479 ± 3 mBq/m^3) are typically a factor of 2–3 lower compared to predominantly continental fetch regions (C1; 1 004 ± 6 mBq/m^3), and "deep baseline" events (DB1; 279 ± 3 mBq/m^3); are a factor of 3–4 smaller again (Table 2). The "mixed zones" (M1 and M2) had atmospheric radon concentrations intermediate between the marine and continental sectors, with M1 having a mean of 725 ± 5 mBq/m^3, and M2 having a mean of 493 ± 3 mBq/m^3.

Inter-annual percentiles of the Cape Point radon data, binned according to the four prominent WD sectors (MA1, M1, M2 and C1), are presented in Fig. 10. A decreasing trend in atmospheric radon was found in region C1 (continental) within the 50th, 75th, and 95th percentiles. Making use of the linear trend lines from C1 for the 5th (R^2 = 0.74), 25th (R^2 = 0.81), 50th (R^2 = 0.85), 75th (R^2 = 0.72), and 95th (R^2 = 0.63) percentiles, the radon decreased by 40%, 47%, 62%, 52% and 31%, respectively (Fig. 10). The trend line of the 95th radon percentile from the mixed region M2 also indicated a decrease over the 15 years of observation. However, the results from the marine air mass region (MA1) and the other mixing region (M1) showed no significant inter-annual trends.

Factors which could potentially contribute to the observed long-term decreasing higher radon percentiles in the continental sectors (Figs. 9 and 10) at the Cape Point Station include changes in (1) airflow patterns (Rayner, 2007; Griffiths et al., 2010; Chambers et al., 2011; McVicar et al., 2012); (2) surface air temperature; (3) rainfall patterns affecting water-table depth and, consequently, soil-moisture content and therefore radon emanations (Griffiths et al., 2010); and (4) mixing depths and removal of radon from the boundary layer by deep convection and frontal systems (Williams et al., 2011). Large-scale regional wind run decreases of more than 25% has been observed from a 30-year study (1974–2005) at 20 climatic stations of the Western Cape (Hoffman et al., 2011). A long term (1974–2012) increase in surface air temperature trends of the Western Cape ranging between 0.01 °C/a (Hoffman et al., 2011) and 0.06 °C/a (Jury, 2013) is evident.

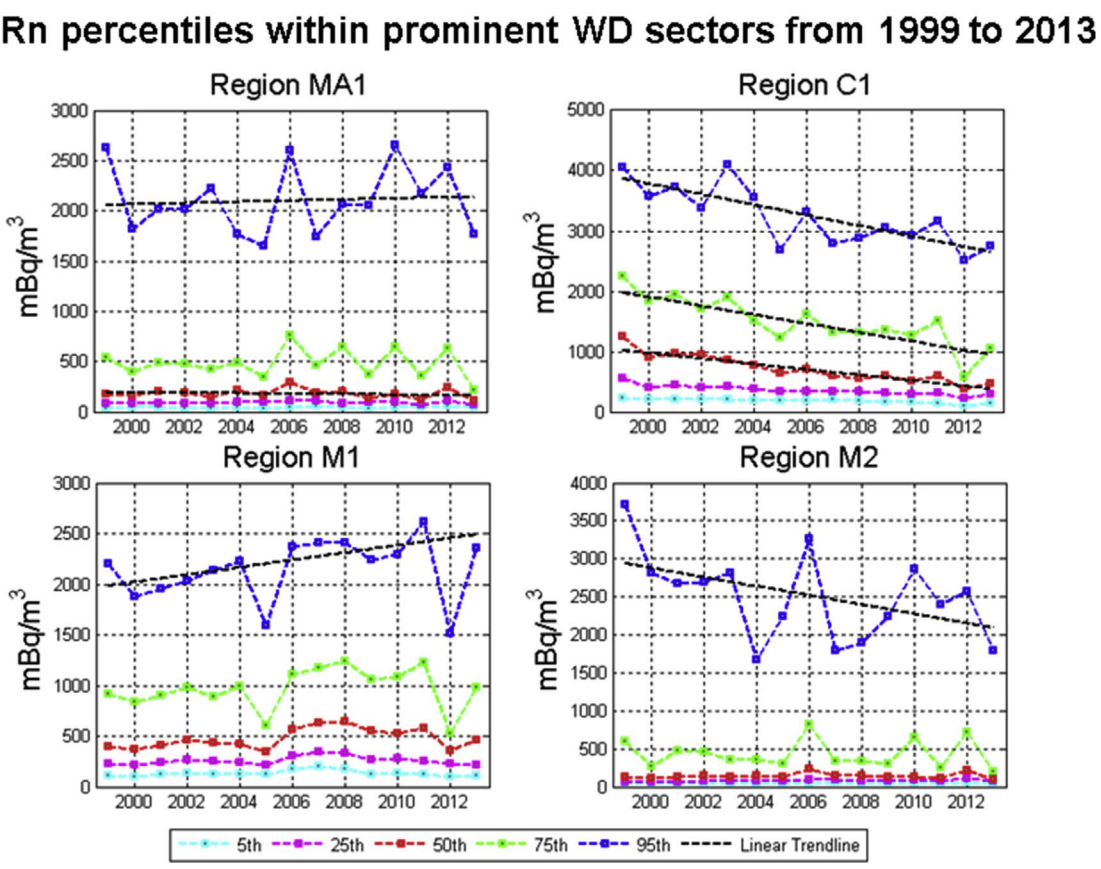
222Rn percentiles within prominent WD sectors from 1999 to 2013
Region MA1
Region C1
Region M1
Region M2
mBq/m3
2000 2002 2004 2006 2008 2010 2012
5th 25th 50th 75th 95th Linear Trendline

Fig. 10. Results of atmospheric radon distributions expressed according to four strategic WD sectors. The radon distributions are characterised by 5th, 25th, 50th, 75th and 95th percentiles with selected linear-trend lines (dashed lines) highlighting certain observed features.

4. Conclusion

Fifteen years of hourly measurements of atmospheric radon concentrations at the low-altitude Southern Hemisphere coastal Cape Point Station are statistically characterised and compared with meteorological data within this study. A mean radon concentration of 676 ± 2 mBq/m^3 was determined over the entire multi-year dataset, superimposed on which was a strong annual cycle with maxima during the winter seasons and minima during the summer seasons. The radon distributions at Cape Point are strongly skewed, with data below the median exhibiting a small range (289 mBq/m^3 between the 5th and 50th percentiles), whereas data above the median has a large range (2 262 mBq/m^3 between the 50th and 95th percentiles). Furthermore, the range in the higher percentiles varies seasonally, with the most elevated atmospheric radon activity concentrations predominantly occurring during the autumn and winter months. Expectedly, the mean atmospheric radon-associated with predominant continental fetch regions (1 004 ± 6 mBq/m^3) was about twice higher compared to oceanic fetch regions (479 ± 3 mBq/m^3). A power spectral FFT analysis of the 15-year radon time series reveals prominent peaks at semi-diurnal, diurnal and annual timescales. The annual peak indicates major seasonal changes in the patterns of offshore versus onshore flow associated with regional/hemispheric circulation patterns, whereas the diurnal and semi-diurnal peaks together reflect the influence of local nocturnal radon build-up over land, and the interplay between mesoscale sea/land breezes. A data decomposition according to wind direction confirmed the conclusion that the observed variations in monthly radon distributions was chiefly due to seasonal switching in the frequency of air masses approaching Cape Point from continental, oceanic and mixed fetch regions. The number of atmospheric radon events observed is strongly dependent on the WD.

An analysis of diurnal composites of radon and wind confirm that winter radon levels are significantly higher than summer due to an increased frequency of winds from the NNW (the so-called “Berg winds”), associated with continental air masses. Whereas there has been little change in summer, winter-time diurnal radon concentrations have significantly reduced over the multi-year data set, with the largest change being around 200 mBq/m^3 (17%) near the mid-morning maximum. This coincides with a clear drop in wind speeds over the entire diurnal cycle, and a shift in direction from NNW towards northerlies or even NNE.

An evident inter-annual decline in the higher radon percentiles (50th, 75th and 95th) for the winter and spring seasons were observed, with most of the change occurring in the first 9 years (1999–2007) of the 15-year data set. An estimated decrease of up to 46% was observed for the 75th radon percentile associated with the winter seasons. An unmistakeable inter-annual decrease for all radon percentiles was detected in air masses from continental fetch regions, with a decrease of 62% in the median concentration over the 15 years of the radon record. By contrast, no significant statistical inter-annual changes were observed in any of the radon percentiles associated with oceanic air masses. This confirms a hypothesis that the observed inter-annual trends in radon concentrations in this data set are predominantly the result of changes in the frequency of air masses arriving at Cape Point from over the African continental land surface. The general decrease of atmospheric radon-associated with continental air-masses at Cape Point from 1999 to 2013 could be attributed to changing meteorological conditions, perhaps driven by climate change.

Acknowledgements

The authors would like to thank the Australian Nuclear Science and Technology Organisation (ANSTO) for supplying the atmospheric radon detectors. The South African National Research Foundation (NRF) is acknowledged for academic funding (MANUS MatSci, Grant No. 109869). We appreciated the technical assistance, data processing, and analyses advice from the ANSTO and SAWS GAW staff. The measurements made at the Cape Point Station are supported by the South African Weather Service.

References

Ball, T.K., Cameron, D.G., Colman, T.B., Roberts, P.D., 1991. Behaviour of radon in the geological environment: a review. Q. J. Eng. Geol. Hydrogeol. 24, 169–182. http://doi.org/10.1144/GSL.QJEG.1991.024.02.01.

Brunke, E.G., Labuschagne, C., Parker, B., Scheel, H.E., Whittlestone, S., 2004. Baseline air mass selection at Cape Point, South Africa: application of 222Rn and other filter criteria to CO2. Atmos. Environ. 38, 5693–5702. http://doi.org/10.1016/j.atmosenv.2004.04.024.

Botha, R., Newman, R.T., Lindsay, R., Maleka, P.P., 2017. Radon and thoron in-air occupational exposure study within selected wine cellars of the Western Cape (South Africa) and associated annual effective doses. Health Phys. 112, 98–107. http://doi.org/10.1097/HP.0000000000000574.

Chambers, S., Williams, A.G., Zahorowski, W., Griffiths, A., Crawford, J., 2011. Separating remote fetch and local mixing influences on vertical radon measurements in the lower atmosphere. Tellus B Chem. Phys. Meteorol 63, 843–859. http://doi.org/10.1111/j.1600-0889.2011.00565.x.

Chambers, S., Zahorowski, W., Williams, A.G., Crawford, J., Griffiths, A., 2013. Identifying tropospheric baseline air masses at Mauna Loa Observatory between 2004 and 2010 using Radon-222 and back trajectories. J. Geophys. Res.: Atmosphere 118, 1–3. http://doi.org/10.1029/2012JD018212.

Chambers, S.D., Hong, S.-B., Williams, A.G., Crawford, J., Griffiths, A.D., Park, S.-J., 2014. Characterising terrestrial influences on Antarctic air masses using Radon-222 measurements at King George Island. Atmos. Chem. Phys. 14, 9903–9916. http://doi.org/10.5194/acp-14-9903-2014.

Chambers, S.D., Williams, A.G., Conen, F., Griffiths, A.D., Reimann, S., Steinbacher, M., Krummel, P.B., Steele, L.P., van der Schoot, M.V., Galbally, I.E., others, 2016. Towards a universal "Baseline" characterisation of air masses for high-and low-altitude observing stations using Radon-222. Aerosol Air Qual. Res 16, 885–899. http://doi.org/10.4209/aaqr.2015.06.0391.

Crawford, J., Zahorowski, W., Cohen, D.D., 2009. A new metric space incorporating radon-222 for generation of back trajectory clusters in atmospheric pollution studies. Atmos. Environ. 43, 371–381. http://doi.org/10.1016/j.atmosenv.2008.09.073.

Florea, N., Duliu, 2012. Eighteen years of continuous observation of Radon and Thoron progenies atmospheric activity. J. Environ. Radioact. 104, 14–23. http://doi.org/10.1016/j.jenvrad.2011.10.002.

Griffiths, A.D., Zahorowski, W., Element, A., Werczynski, S., 2010. A map of radon flux at the Australian land surface. Atmos. Chem. Phys. 10, 8969–8982. http://doi.org/10.5194/acp-10-8969-2010.

Griffiths, A.D., Chambers, S.D., Williams, A.G., Werczynski, S., 2016. Increasing the accuracy and temporal resolution of two-filter radon–222 measurements by correcting for the instrument response. Atmos. Meas. Tech 9, 2689–2707. http://doi.org/10.5194/amt-9-2689-2016.

Hoffman, M.T., Cramer, M.D., Gillson, L., Wallace, M., 2011. Pan evaporation and wind run decline in the Cape Floristic Region of South Africa (1974–2005): implications for vegetation responses to climate change. Clin. Chem. 109, 437–452. http://doi.org/10.1007/s10584-011-0030-z.

Jury, M.R., 2013. Climate trends in southern Africa. S. Afr. J. Sci. 109, 980–991. https://doi.org/10.1590/sajs.2013/980.

Karstens, U., Schwingshackl, C., Schmithüsen, D., Levin, I., 2015. A process-based 222Rn flux map for Europe and its comparison to long-term observations. Atmos. Chem. Phys. 15, 12845–12865. http://doi.org/10.5194/acp-15-12845-2015.

McVicar, T.R., Roderick, M.L., Donohue, R.J., Li, L.T., Van Niel, T.G., Thomas, A., Grieser, J., Jhajharia, D., Himri, Y., Mahowald, N.M., Mescherskaya, A.V., Kruger, A.C., Rehman, S., Dinpashoh, Y., 2012. Global review and synthesis of trends in observed terrestrial near-surface wind speeds: implications for evaporation. J. Hydrol. 416–417, 182–205. http://doi.org/10.1016/j.jhydrol.2011.10.024.

Rayner, D.P., 2007. Wind run changes: the dominant factor affecting pan evaporation trends in Australia. J. Clim. 20, 3370–3394. http://doi.org/10.1175/JCLI4181.1.

Schery, S.D., Huang, S., 2004. An estimate of the global distribution of radon emissions from the ocean. Geophys. Res. Lett. 31. http://doi.org/10.1029/2004GL021051.

Slemr, F., Brunke, E.G., Whittlestone, S., Zahorowski, W., Ebinghaus, R., Kock, H.H., Labuschagne, C., 2013. 222Rn-calibrated mercury fluxes from terrestrial surface of southern Africa, in: atmospheric Chemistry and Physics. pp. 6421–6428. http://doi.org/10.5194/acp-13-6421-2013.

Whittlestone, S., Kowalczyk, E., Brunke, E.-G., Labuschagne, C., 2009. Source regions for CO2 at Cape Point assessed by modelling, 222Rn and meteorological data, South African Weather Service, Pretoria, South Africa, ISBN 978-0-9584463-9-6.

Whittlestone, S., Zahorowski, W., 1998. Baseline radon detectors for shipboard use: development and deployment in the first aerosol characterization experiment (ACE 1). J. Geophys. Res. 103, 16743–16751. http://doi.org/10.1029/98JD00687.

Williams, A.G., Zahorowski, W., Chambers, S., Griffiths, A., Hacker, J.M., Element, A., Werczynski, S., 2011. The vertical distribution of radon in clear and cloudy daytime terrestrial boundary layers. J. Atmos. Sci. 68, 155–174. http://doi.org/10.1175/2010JAS3576.1.

Zahorowski, W., Chambers, S.D., Henderson-Sellers, A., 2004. Ground based radon-222 observations and their application to atmospheric studies. J. Environ. Radioact. 76, 3–33. http://doi.org/10.1016/j.jenvrad.2004.03.033.

Zahorowski, W., Griffiths, A.D., Chambers, S.D., Williams, A.G., Law, R.M., Crawford, J., Werczynski, S., 2013. Constraining annual and seasonal radon-222 flux density from the Southern Ocean using radon-222 concentrations in the boundary layer at Cape Grim. Tellus B 65. http://doi.org/10.3402/tellusb.v65i0.19622.